NEAR-FIELD INFRARED SPECTROSCOPY OF ORDINARY CHONDRITES: NEW INSIGHTS INTO MINERAL AND ORGANIC COMPONENTS. T. D. Glotch[1], J. M. Young[1], Z. Yao[1,2], and H. A. Bechtel[2], [1]Stony Brook University, Stony Brook, NY (timothy.glotch@stonybrook.edu), [2]Advanced Light Source, Lawrence Berkeley National Laboratory, Berkeley, CA.

Introduction: The relationships between organic and mineral components in meteorite have been a topic of extensive study [e.g., 1-3]. We have previously used the Raman spectral properties of the disordered and graphitic (D and G) bands of polycyclic aromatic hydrocarbons (PAHs) to constrain the peak metamorphic temperatures experienced by a range of ordinary chondrite samples [4]. We found two populations of organic carbon in these samples that appear to reflect different thermal histories. In this work we use scattering-type scanning near field infrared spectroscopy and imaging (s-SNOM or nano-FTIR) to investigate organic/silicate boundaries in H5 ordinary chondrite ALH77012 at ~20 nm spatial scales.

Methods: We acquired nano-FTIR spectra and images at the Synchrotron Infrared Nano Spectroscopy (SINS) beamline at the Advanced Light Source at Lawrence Berkeley National Laboratory. For spectroscopy, the synchrotron infrared beam was focused on to a conductive atomic force microscope (AFM) tip in a neaspec neaSNOM near-field system. Phase and amplitude spectra referenced to a gold standard were collected at harmonics of the AFM tip tapping frequency to remove the far-field signal. The spatial resolution of point spectroscopy measurements is controlled by the radius of curvature of the AFM tip, which is < 20 nm.

For imaging, a tunable laser centered at ~6 µm was used to illuminate the sample tip as it rastered over the sample. The image was acquired with a spatial sampling of 53 nm/pixel. As with the spectroscopic measurements, near-field infrared phase and amplitude data were collected at harmonics of the tapping frequency.

Results and Discussion: Using Raman maps collected by [4] at Stony Brook University as guides, we focused our nano-IR measurements on organic/silicate boundaries in the H5 ordinary chondrite ALH77012. Figure 1 shows a 6 µm nano-IR map of one of these boundaries. From the multiple datatypes that were collected simultaneously, we constructed an overlay of colorized optical amplitude (O3A) at a wavelength of 6 µm over the mechanical phase (M1P). The map shows a clear boundary trending from lower left to upper right. The upper portion of the image (yellow/white) has weak or absent spectral features between ~700 and 1200 cm^{-1}. The amplitude spectrum shows a broad peak centered at ~1220 cm^{-1} while the phase spectrum is flat in this region. Given the lack of diagnostic spectral features in this wavelength range as well as the high reflectance of the material in reflected light micrographs, we interpret this phase to be a metal sulfide or oxide.

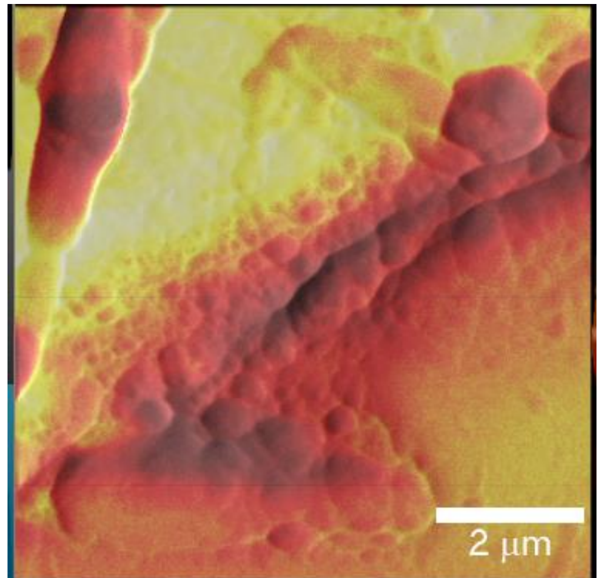

Figure 1. Overlay of the near-field amplitude at 6 µm (O3A) on the mechanical phase (M1P). Red/dark tones indicate lower amplitudes and yellow/bright tones indicate higher amplitude.

We collected multiple spectra on the Raman-identified organic material (displayed as red/orange in Figure 1). Multiple diagnostic features are present, in both the phase and amplitude spectra, although there is some variation from point to point. Major peaks in the phase spectra occur at ~880, 974, 1010, 1074, 1120, and 1290 cm^{-1}. Corresponding peaks in the amplitude spectra occur at ~860, 950, 1009, 1054, 1114 cm^{-1}, and 1280 cm^{-1}. Most of these features correspond to pyroxene Si-O stretching and bending modes, although the shortest wavelength (highest wavenumber) feature is absent from spectra of pyroxene standards, and may correspond to weak features documented in some PAH spectra [5]. Future work will include refinement of band identifications and investigations of additional mineral and organic features in ALH77012 and other ordinary chondrites.

References: [1] Sephton et al. (2002), PSS, 50, 711-716. [2] Quirico et al. (2003), MAPS, 38, 795-811. [3] Cloutis et al. (2016), Icarus, 274, 211-230. [4] Young & Glotch (2019), LPSC L, abstract 1860. [5] Bernstein et al. (2005), ApJSS, 161, 53-64.